2019

Knowledge-Aided Target Detection for Multistatic Passive Radar

Guohao Sun
University of Electronic Science and Technology of China

Wei Zhang
University of Electronic Science and Technology of China

Jun Tong
University of Wollongong, jtong@uow.edu.au

Zishu He
University of Electronic Science and Technology of China

Zhihang Wang
University of Electronic Science and Technology of China

Knowledge-Aided Target Detection for Multistatic Passive Radar

Abstract

This paper studies the detection problem for multistatic passive radar. We consider scenarios where prior knowledge about the spectrum and peak-to-average ratio (PAR) of the non-cooperative illuminators of opportunity (IOs) is available. We develop several knowledge-aided (KA) detectors within the framework of the generalized likelihood ratio test (GLRT) to exploit such prior knowledge. Particularly, the knowledge about the bandwidth of the transmitted signal is employed to suppress the out-of-band noise, and the knowledge about the PAR constraint is exploited to eliminate the remaining high-power noise. The challenge of unknown spectrum condition is also addressed, where block sparse Bayesian learning (BSBL) is exploited to derive the maximum-likelihood estimates (MLEs) of the unknown, temporally correlated signal. The numerical results indicate that the proposed KA detectors offer significant performance improvements compared with the traditional detectors, which do not exploit such prior information.

Publication Details

G. Sun, W. Zhang, J. Tong, Z. He & Z. Wang, "Knowledge-Aided Target Detection for Multistatic Passive Radar," IEEE Access, vol. 7, pp. 53463-53475, 2019.

IEEE Access
Multidisciplinary | Rapid Review | Open Access Journal

Received March 15, 2019, accepted April 11, 2019, date of publication April 18, 2019, date of current version May 2, 2019.

Digital Object Identifier 10.1109/ACCESS.2019.2911910

Knowledge-Aided Target Detection for Multistatic Passive Radar

GUOHAO SUN[1], (Student Member, IEEE), WEI ZHANG[1], JUN TONG[2], (Member, IEEE), ZISHU HE[1], (Member, IEEE), AND ZHIHANG WANG[1], (Student Member, IEEE)

[1]School of Information and Communication Engineering, University of Electronic Science and Technology of China, Chengdu 611731, China
[2]School of Electrical, Computer and Telecommunications Engineering, University of Wollongong, Wollongong, NSW 2522, Australia

Corresponding author: Wei Zhang (5282411@qq.com)

This work was supported by the National Natural Science Foundation of China under Grant 61671137, Grant 61401062, and Grant 61771095.

ABSTRACT This paper studies the detection problem for multistatic passive radar. We consider scenarios where prior knowledge about the spectrum and peak-to-average ratio (PAR) of the non-cooperative illuminators of opportunity (IOs) is available. We develop several knowledge-aided (KA) detectors within the framework of the generalized likelihood ratio test (GLRT) to exploit such prior knowledge. Particularly, the knowledge about the bandwidth of the transmitted signal is employed to suppress the out-of-band noise, and the knowledge about the PAR constraint is exploited to eliminate the remaining high-power noise. The challenge of unknown spectrum condition is also addressed, where block sparse Bayesian learning (BSBL) is exploited to derive the maximum-likelihood estimates (MLEs) of the unknown, temporally correlated signal. The numerical results indicate that the proposed KA detectors offer significant performance improvements compared with the traditional detectors, which do not exploit such prior information.

INDEX TERMS Target detection, multistatic passive radar, knowledge-aided detection, generalized likelihood ratio test (GLRT).

I. INTRODUCTION

Passive radar exploits noncooperative and readily available illuminators of opportunity (IOs) to detect and track targets of interests. Without an active transmitter, passive radar possesses the advantages of low implementation costs, stealth, and ability to avoid interference [1]–[6] and has wide applications in military and civilian scenarios. For example, [2], [3] study vehicular passive radar utilizing indoor WiFi signals to monitor indoor area. In [7], passive radar is exploited to protect the route safety through detecting potential dangerous aerial vehicles and birds around the airport. In urban sensing applications, passive radar is used in traffic control by relying on the existing high-power communication signals as a potential IO to detect and track vehicles. This avoids influencing the existing communication equipments as the radar does not actively transmit signals.

In general, passive radar systems can be classified into two categories according to whether a reference path (RP) (i.e., the direct transmitter-radar path) is employed [8]–[11]. The first category utilizes only the surveillance paths (SP) (i.e., the transmitter-target-radar path) to detect the potential target signal while ensuring that the null of the antenna array is steered towards the transmitter [8]. The other category use the SP and RP jointly: The echoes from the RP can be collected first as the prior information and then the echoes from the SP and RP are jointly exploited to detect targets. In this category, the prior information from RP is well leveraged to avoid its strong impact on target detection. According to the number of distributed receivers, passive radars may also be classified into multistatic or monostatic systems [11]–[14]. Compared with monostatic systems, multistatic passive radar can potentially improve the detection performance with more degrees of freedom [15]. Furthermore, multistatic passive radar is able to reduce the influence of target scintillations caused by spatial properties of the targets' radar cross section (RCS). Therefore, distributed passive radars may benefit from the enhanced spatial or geometric diversity to improve target detection, as a result of statistically independent observations of the targets from different spatial angles [16].

It is of significant importance to sufficiently exploit the low-power, non-cooperative signals from IOs for passive radar. Fortunately, for passive radar systems that exploit communications signals, e.g., from broadcast stations, mobile

The associate editor coordinating the review of this manuscript and approving it for publication was Hasan S. Mir.

stations, and WiFi signals [17], [18], a prior knowledge about the signal can be available. In particular, the bandwidth may be used to suppress the noise and thus improve the ability of detection [19]. Moreover, the peak-to-average ratio (PAR), which is often controlled in communication systems [20] to maintain the efficiency of power amplifiers and reduce the out-of-band radiation, may help improve the estimate of the transmitted signal. Exploiting such prior knowledge may compensate for the loss due to the lack of cooperation in passive radar and effectively improve the detection performance [21], [22]. To the best of our knowledge, such knowledge has not been exploited in the past studies in the open literature. Consequently, the estimation of the unknown signal can suffer significantly from noise, which may in turn lead to a poor performance of the "cross-correlation" (CC) detector [23]–[25].

In this paper, we investigate how to exploit the prior knowledge about the bandwidth and PAR and develop knowledge-aided (KA) detectors for multistatic passive radar with noisy SPs and RPs. We resort to a generalized likelihood ratio test (GLRT) and propose several bandwidth- and PAR-based KA detectors. Two KA detectors are proposed for the case where both the bandwidth and PAR constraints are considered, based on the power method and cyclic optimization, respectively. We further discuss two detectors for constant modulus signals, by applying upper and lower bounds to the optimization problem. We also discuss the case where knowledge about the bandwidth or PAR only is available and show that the bandwidth knowledge can be exploited to suppress a majority of noise and the PAR constraint can eliminate the higher powered noise, which improves the accuracy of the transmitting signal estimation. In addition, the sparse Bayesian learning (SBL) algorithm is utilized to tackle the case where the bandwidth is unknown. The proposed detectors are evaluated for the distributed passive radar system in different scenarios, which shows notable improvement over the traditional detectors that do not exploit prior knowledge.

The rest of this paper is organized as follows: Section II describes the signal model and formulates the detection problem for multistatic passive radar systems. Section III introduces the proposed GLRT-based detectors that exploit the bandwidth and PAR knowledge. Section IV introduces several special cases and also addresses the case with unknown bandwidth. Simulations and analysis of the proposed detectors are given in Section V. Finally, conclusions are drawn in Section VI.

Notation: $\mathbb{R}^n$ and $\mathbb{C}^n$ denote the n-dimensional real and complex vector space, respectively. $\mathbb{R}^{m\times n}$ and $\mathbb{C}^{m\times n}$ denote the $m\times n$-dimensional real and complex matrix space, respectively. $(\cdot)^T$, $(\cdot)^*$, $(\cdot)^\dagger$, vec$(\cdot)$, and $\lambda_{max}(\cdot)$ denote the transpose, complex conjugate, conjugate transpose, vectorization, and largest eigenvalue, respectively. $|\cdot|$ denotes the modulus of a complex scalar. $\|\cdot\|$ denotes the ℓ_2 norm of a vector. $\|\cdot\|_F$ denotes the Frobenius norm of a matrix. $\otimes$ denotes the Kronecker product. $R(\mathbf{H})$ denotes the range space of matrix $\mathbf{H}$. Re$(\cdot)$ denotes the real part of a scalar, vector or matrix.

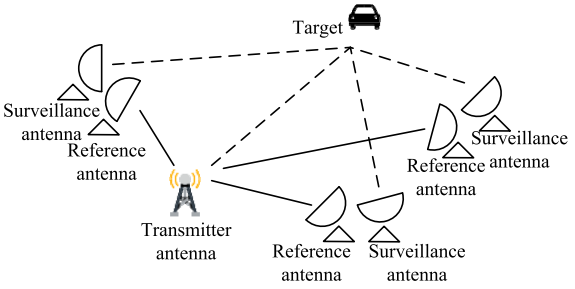

FIGURE 1. Configuration of a multistatic passive radar system with colocated reference and surveillance antennas.

II. SIGNAL MODEL AND PROBLEM FORMULATION

Consider a multistatic passive radar system that employs M distributively located stations, as shown schematically in Fig. 1. Colocated reference and surveillance antennas are deployed at each station, where the reference antennas point to the transmitter while the surveillance antennas are steered toward the direction to be surveyed. Assume that the signals from the two paths are synchronized such that the relative delay can be ignored, which may be achieved by estimating the time delays and matched filtering. We assume that multipath, clutter and direct path signal can be removed by some developed technologies, such as Digital Beam Forming technology, Kalman filter in tracking method.

Assume that the signal is received and sampled by frequency f_0. Besides, we assume that different surveillance and reference receivers use a same clock and collect all received signals into a centralized signal processing station. The received noise spread along whole spectrum compared transmit signal and it is drawn from the circular Gaussian distribution [4], [26]–[28]. Therefore, the hypothesis testing problem can be formulated as

$$H_0: \begin{cases} \mathbf{Y}_r = \mathbf{s}\boldsymbol{\alpha}^T + \mathbf{W}_r \\ \mathbf{Y}_s = \mathbf{W}_s \end{cases} \qquad H_1: \begin{cases} \mathbf{Y}_r = \mathbf{s}\boldsymbol{\alpha}^T + \mathbf{W}_r \\ \mathbf{Y}_s = \mathbf{s}\boldsymbol{\beta}^T + \mathbf{W}_s, \end{cases} \tag{1}$$

where

- $\mathbf{Y}_r = \left[\mathbf{y}_{r,1}, \mathbf{y}_{r,2}, \ldots, \mathbf{y}_{r,M}\right] \in \mathbb{C}^{N\times M}$ denotes the received signals from the RPs,
- $\mathbf{Y}_s = \left[\mathbf{y}_{s,1}, \mathbf{y}_{s,2}, \ldots, \mathbf{y}_{s,M}\right] \in \mathbb{C}^{N\times M}$ denotes the received signals from the SPs,
- $\mathbf{y}_{r,m} = \left[y_{r,m}[1], y_{r,m}[2], \ldots, y_{r,m}[N]\right]^T$,
- $\mathbf{y}_{s,m} = \left[y_{s,m}[1], y_{s,m}[2], \ldots, y_{s,m}[N]\right]^T$,
- $\boldsymbol{\alpha} = [\alpha_1, \alpha_2, \ldots, \alpha_M]^T$ denotes the attenuation on RP,
- $\boldsymbol{\beta} = [\beta_1, \beta_2, \ldots, \beta_M]^T$ denotes the attenuation and the RCS of the target to be detected,
- $\mathbf{s} = [s[1], s[2], \ldots, s[N]]^T$ denotes the unknown signal of opportunity,
- $\mathbf{W}_r$ and $\mathbf{W}_s$ denote the matrices of noise whose power σ_m^2 is assumed having the same noise power for

simplifying derivations and also assumed equal for each pair of RP and SP, and we define as $\mathbf{W} = [\mathbf{w}_1, \mathbf{w}_2, \ldots, \mathbf{w}_M]$,
- N denotes the length of observations, which is determined by the sampling rate and bandwidth.

Previous works do not consider any prior knowledge about the signal $\mathbf{s}$, and the CC detector is given by

$$\sum_{m=1}^{M} \left| \mathbf{y}_{r,m}^{\dagger} \mathbf{y}_{s,m} \right| \underset{H_0}{\overset{H_1}{\gtrless}} \xi, \tag{2}$$

where we use ξ to denote the generic detection threshold. The performance of this detector may degrade when the RP or SP are severely noisy. Note that in the remainder of this paper, we reuse ξ to denote the threshold of a detector, whose value may vary with the detectors.

We may employ prior knowledge about the unknown signal $\mathbf{s}$ to improve the detection performance. Consider the spectra decomposition of $\mathbf{s}$:

$$\mathbf{s} = \tilde{\mathbf{H}}\tilde{\mathbf{x}}, \tag{3}$$

where

$$\tilde{\mathbf{H}} = [\mathbf{a}(f_1), \mathbf{a}(f_2), \ldots, \mathbf{a}(f_N)] \in \mathbb{C}^{N \times N} \tag{4}$$

is the $N \times N$ Fourier transform matrix with $\mathbf{a}(f_i) = \left[1, e^{-j2\pi f_i}, \cdots, e^{-j2\pi f_i(N-1)}\right]$, $i = 1, 2, \cdots, N$ where $f_i = \frac{i-1}{N}$ is the normalized frequency, and $\tilde{\mathbf{x}}$ denotes the corresponding Fourier coefficient vector. The opportunity signal usually originates from the broadcasting stations, mobile stations, etc, and occupies a fixed frequency band with a certain bandwidth. Assume that a band limited signal $\mathbf{s}$ with frequency domain from f_{s1} to f_{s2}. We can normalize it by f_0, and we can obtain signal $\mathbf{s}$ by Fourier matrix $[\mathbf{a}(f_{s1}/f_0), \cdots, \mathbf{a}(f_{s2}/f_0)]$. We define the number of columns of the matrix is B. Therefore, we can impose a bandwidth constraint on the unknown signal by assuming the following subspace model [5]

$$\mathbf{s} = \mathbf{H}\mathbf{x}, \tag{5}$$

where $\mathbf{x}$ is a $B \times 1$ coefficient vector and $B < N$ is the dimension of the subspace. In this way, a bandwidth constraint is imposed on the unknown signal $\mathbf{x}$ which can be uniquely represented by $\mathbf{x}$. Note that the matrix $\mathbf{H} \in \mathbb{C}^{N \times B}$ can be comprised of the Fourier matrix. Besides, $\mathbf{H}$ can also be other prior spectrum based matrix. The value B also means the rank of basis matrix $\mathbf{H}$. When $B = N$, the matrix $\mathbf{H}$ is nonsingular and the received signal vector $\mathbf{s}$ spreads the whole spectrum.

Furthermore, we may incorporate the prior knowledge about the PAR into the multistatic passive radar detection problem, which is defined as [29]

$$\rho(\mathbf{s}) = \frac{\max_n |s[n]|^2}{\|\mathbf{s}\|^2/N}. \tag{6}$$

Clearly, $\rho(\mathbf{s})$ is always equal to or greater than 1.

III. KA DETECTORS WITH PRIOR KNOWLEDGE ABOUT BANDWIDTH AND PAR

As mentioned earlier, the prior knowledge about the unknown signal $\mathbf{s}$ may be obtained in various ways. In this section, we investigate how to exploit the bandwidth and PAR information for detecting targets in multistatic passive radar systems. Our treatments are based on the GLRT framework by replacing unknown parameters with their maximum likelihood estimates (MLEs). Two detectors employing the power method and cyclic optimization will be presented. The special case of constant-modulus transmitted signals will be treated using upper and lower bound methods.

We first study how to detect targets with a PAR constraint $\rho(\mathbf{s}) \leq \gamma$ and bandwidth constraint (i.e., $\mathbf{s} = \mathbf{H}\mathbf{x}$), where γ is a constant. Adopting the MLEs of the unknown parameters, the GLRT problem is formulated as

$$\frac{\max\limits_{\boldsymbol{\alpha},\boldsymbol{\beta},\mathbf{s}\in R(\mathbf{H}),\rho(\mathbf{s})\leq\gamma} p_1(\mathbf{Y}_r, \mathbf{Y}_s|\boldsymbol{\alpha}, \boldsymbol{\beta}, \mathbf{s})}{\max\limits_{\boldsymbol{\alpha},\mathbf{s}\in R(\mathbf{H}),\rho(\mathbf{s})\leq\gamma} p_0(\mathbf{Y}_r, \mathbf{Y}_s|\boldsymbol{\alpha}, \mathbf{s})} \underset{H_0}{\overset{H_1}{\gtrless}} \xi, \tag{7}$$

where $R(\mathbf{H})$ denotes the range space of $\mathbf{H}$ and the conditional probability density function (PDF) $p_i(\mathbf{Y}_r, \mathbf{Y}_s|\boldsymbol{\alpha}, i\boldsymbol{\beta}, \mathbf{s})$ is assumed to follow a normal distribution as

$$\begin{aligned} &p_i(\mathbf{Y}_r, \mathbf{Y}_s|\boldsymbol{\alpha}, i\boldsymbol{\beta}, \mathbf{s}) \\ &= \prod_{m=1}^{M} \frac{1}{\pi^{2N}\sigma_m^{4N}} \\ &\quad \times \exp\left\{-\frac{1}{\sigma_m^2}\left[\|\mathbf{y}_{s,m} - i\beta_m\mathbf{s}\|^2 + \|\mathbf{y}_{r,m} - \alpha_m\mathbf{s}\|^2\right]\right\}, \end{aligned} \tag{8}$$

with $i = 0$ and 1 for hypotheses H_0 and H_1, respectively. By eliminating some constant terms, the GLRT in (7) can be simplified to

$$\begin{aligned} \min_{\boldsymbol{\alpha},\mathbf{s}\in R(\mathbf{H}),\rho(\mathbf{s})\leq\gamma} &\sum_{m=1}^{M} \|\mathbf{n}_{0,m}\|^2 \\ &- \min_{\boldsymbol{\alpha},\boldsymbol{\beta},\mathbf{s}\in R(\mathbf{H}),\rho(\mathbf{s})\leq\gamma} \sum_{m=1}^{M} \|\mathbf{n}_{1,m}\|^2 \underset{H_0}{\overset{H_1}{\gtrless}} \xi, \end{aligned} \tag{9}$$

where

$$\begin{aligned} \|\mathbf{n}_{0,m}\|^2 &= \frac{1}{\sigma_m^2}\left\|[\mathbf{y}_{s,m}, \mathbf{y}_{r,m}] - [\mathbf{0}_N, \alpha_m\mathbf{s}]\right\|^2 \\ \|\mathbf{n}_{1,m}\|^2 &= \frac{1}{\sigma_m^2}\left\|[\mathbf{y}_{s,m}, \mathbf{y}_{r,m}] - [\beta_m\mathbf{s}, \alpha_m\mathbf{s}]\right\|^2. \end{aligned} \tag{10}$$

The two minimization problems in (9) do not admit closed-form solutions. We here provide two methods. One is based on the power method with bandwidth constraint (PARPBC) [30] and the other is the PAR cyclic optimization with bandwidth constraint (PARCBC), which jointly estimate α_m, β_m and $\mathbf{s}$. The special case of unit PAR is also treated by using two algorithms, i.e., the PARloBC and PARupBC, based on upper bounding and lower bounding, respectively.

A. PARPBC DETECTOR

Plugging in the MLEs of the unknown amplitudes and incorporating the low-rank constraint, the GLRT problem of (9) can be reduced as (see Appendix VI for details)

$$\max_{\mathbf{s},\rho(\mathbf{s})\le\gamma} \frac{\mathbf{s}^\dagger \mathbf{P}_H \mathbf{R}_1 \mathbf{P}_H \mathbf{s}}{\mathbf{s}^\dagger \mathbf{s}} - \max_{\mathbf{s},\rho(\mathbf{s})\le\gamma} \frac{\mathbf{s}^\dagger \mathbf{P}_H \mathbf{R}_0 \mathbf{P}_H \mathbf{s}}{\mathbf{s}^\dagger \mathbf{s}} \underset{H_0}{\overset{H_1}{\gtrless}} \xi, \tag{11}$$

where

$$\begin{aligned}
\mathbf{P}_H &= \mathbf{H}(\mathbf{H}^\dagger\mathbf{H})^{-1}\mathbf{H}^\dagger \\
\mathbf{R}_0 &= \sum_{m=1}^{M} \tilde{\mathbf{y}}_{r,m}\tilde{\mathbf{y}}_{r,m}^\dagger = \tilde{\mathbf{Y}}_r\tilde{\mathbf{Y}}_r^\dagger \\
\mathbf{R}_1 &= \sum_{m=1}^{M} \left(\tilde{\mathbf{y}}_{s,m}\tilde{\mathbf{y}}_{s,m}^\dagger + \tilde{\mathbf{y}}_{r,m}\tilde{\mathbf{y}}_{r,m}^\dagger\right) = \tilde{\mathbf{Y}}_s\tilde{\mathbf{Y}}_s^\dagger + \tilde{\mathbf{Y}}_r\tilde{\mathbf{Y}}_r^\dagger,
\end{aligned} \tag{12}$$

and we have restructured the vectors and matrices as

$$\begin{aligned}
\tilde{\mathbf{y}}_{r,m} &= \mathbf{y}_{r,m}/\sigma_m \\
\tilde{\mathbf{y}}_{s,m} &= \mathbf{y}_{s,m}/\sigma_m \\
\tilde{\mathbf{Y}}_r &= \left[\tilde{\mathbf{y}}_{r,1}, \tilde{\mathbf{y}}_{r,2}, \ldots, \tilde{\mathbf{y}}_{r,M}\right] \in \mathbb{C}^{N\times M} \\
\tilde{\mathbf{Y}}_s &= \left[\tilde{\mathbf{y}}_{s,1}, \tilde{\mathbf{y}}_{s,2}, \ldots, \tilde{\mathbf{y}}_{s,M}\right] \in \mathbb{C}^{N\times M}.
\end{aligned} \tag{13}$$

The maximization problems in (11) can be reformulated as

$$\begin{aligned}
&\max_{\mathbf{s}} \ \mathbf{s}^\dagger \mathbf{P}_H \mathbf{R}_i \mathbf{P}_H \mathbf{s} \\
&s.t.\ \rho(\mathbf{s}) \le \gamma, \quad \|\mathbf{s}\|^2 = 1,
\end{aligned} \tag{14}$$

for $i = 0$ or 1. This can be solved iteratively by solving a sequence of nearest-vector problems

$$\begin{aligned}
&\min_{\mathbf{s}^{(k+1)}} \ \|\mathbf{s}^{(k+1)} - \mathbf{P}_H \mathbf{R}_i \mathbf{P}_H \mathbf{s}^{(k)}\|^2 \\
&s.t.\ \rho(\mathbf{s}^{(k+1)}) \le \gamma, \quad \|\mathbf{s}^{(k+1)}\|^2 = 1,
\end{aligned} \tag{15}$$

where k is the number of iterations, $\mathbf{s}^{(k)}$ denotes the value of $\mathbf{s}$ at the k-th iteration, and the detailed solution is shown in Appendix VI. The iteration is terminated when $\|\mathbf{s}^{(k+1)} - \mathbf{s}^{(k)}\|^2 < \varepsilon$, where ε is a threshold small enough to guarantee convergence.

Using the estimation method above, it can be shown that the final PARPBC test can be formulated as

$$\frac{\hat{\mathbf{s}}_1^\dagger \mathbf{P}_H \mathbf{R}_1 \mathbf{P}_H \hat{\mathbf{s}}_1}{\hat{\mathbf{s}}_1^\dagger \hat{\mathbf{s}}_1} - \frac{\hat{\mathbf{s}}_0^\dagger \mathbf{P}_H \mathbf{R}_0 \mathbf{P}_H \hat{\mathbf{s}}_0}{\hat{\mathbf{s}}_0^\dagger \hat{\mathbf{s}}_0} \underset{H_0}{\overset{H_1}{\gtrless}} \xi, \tag{16}$$

where $\hat{\mathbf{s}}_1$ and $\hat{\mathbf{s}}_0$ are the solutions of (14) obtained under the hypotheses H_1 and H_0, respectively. The proposed PARPBC detector is summarized in Algorithm 1.

Remark 1: $\mathbf{P}_H$ is equivalent to a bandpass filter with bandwidth B, which allows to suppress the out-of-band noise. Consider a mismatched situation where the true signal bandwidth B' is less than the filter bandwidth, i.e., $B' < B$. After bandpass filtering, the transmitted signal can fully pass the filter but the noise can be suppressed. The signal-to-noise ratio (SNR) of one path is $\frac{\|\mathbf{s}\|^2}{B\sigma_m^2}$, which improves as B approaches B' due to the decrease of the noise level. For the case $B' > B$, the SNR becomes $\frac{\|\mathbf{P}_H\mathbf{s}\|^2}{B\sigma_m^2}$. As B decreases, both the noise and signal levels decrease.

Algorithm 1 PARPBC Test

Step A: Estimate $\hat{\mathbf{s}}_i$ under H_i for $i = 0, 1$:
Input: $\mathbf{R}_i$, the PAR γ and bandwidth matrix $\mathbf{P}_H$.
1: Set k as the number of iterations. Initialize $k = 0$ and set $\mathbf{s}_i^{(0)}$ to be an all-one vector.
2: **while** $\|\mathbf{s}_i^{(k+1)} - \mathbf{s}_i^{(k)}\|^2 > \varepsilon$ **do**
3: Update $\mathbf{s}_i^{(k+1)}$ using the method of (15). $k \leftarrow k + 1$;
4: **end while**
Step B: Conduct the test of (16).

B. PARCBC DETECTOR

The objective function of (9) is convex with respect to α_m, β_m and $\mathbf{s}$, respectively, and thus at least a local optimum can be guaranteed. In the following, we discuss the iterative PARCBC algorithm as summarized in Algorithm 2, which optimizes part of unknown parameters alternatively while the others keep fixed.

Algorithm 2 PARCBC Test

Step A: Estimate $\mathbf{s}_i$ under H_i for $i = 0, 1$:
Input: $\mathbf{Y}_i$, the PAR γ and bandwidth matrix $\mathbf{P}_H$.
1: Set k as the number of iterations. Initialize $k = 0$ and set $\mathbf{s}_i^{(0)}$ to be an all-one vector.
2: **while** $\|\mathbf{s}_i^{(k+1)} - \mathbf{s}_i^{(k)}\|^2 > \varepsilon$ **do**
3: Update $\beta_m^{(k)}$ and $\alpha_m^{(k)}$ by (17) for all m.
4: Update $\tilde{\mathbf{s}}_i^{(k+1)}$ by (19).
5: Calculate $c_i^{(k+1)}$ by (20) and $\mathbf{s}_i^{(k+1)}$ by (21).
6: **end while**
Step B: Conduct the test of (22).

Let $\mathbf{s}^{(k)}, \alpha_m^{(k)}, \beta_m^{(k)}$ be the values of the unknown parameters at the kth iteration. For a fixed $\mathbf{s}^{(k)}$, the MLEs of α_m and β_m are given by (54) and included here for convenience

$$\hat{\beta}_m^{(k)} = \frac{(\mathbf{s}^{(k)})^\dagger \mathbf{y}_{s,m}}{(\mathbf{s}^{(k)})^\dagger \mathbf{s}^{(k)}}, \quad \hat{\alpha}_m^{(k)} = \frac{(\mathbf{s}^{(k)})^\dagger \mathbf{y}_{r,m}}{(\mathbf{s}^{(k)})^\dagger \mathbf{s}^{(k)}}, \tag{17}$$

where $\hat{\beta}_m^{(k)}$ is used only under the H_1 hypothesis. Let $\mathbf{s}^{(k)} = c^{(k)}\tilde{\mathbf{s}}^{(k)}$, where $\tilde{\mathbf{s}}^{(k)}$ denotes the signal with PAR constraint $\rho(\mathbf{s}^{(k)}) \le \gamma$ and $\|\mathbf{s}^{(k)}\|^2 = c^{(k)}$. For fixed $\{\alpha_m^{(k)}\}$ and $\{\beta_m^{(k)}\}$, each of the minimization problems in (9) is equivalent to

$$\begin{aligned}
\min_{\tilde{\mathbf{s}},c} \ & -2\sqrt{c}\mathrm{Re}\left\{\sum_{m=1}^{M} \mathbf{P}_H\left(i\mathbf{y}_{s,m}^\dagger\beta_m^{(k)} + \mathbf{y}_{r,m}^\dagger\alpha_m^{(k)}\right)\tilde{\mathbf{s}}\right\} \\
& + \sum_{m=1}^{M}\left(i|\beta_m^{(k)}|^2 + |\alpha_m^{(k)}|^2\right)c \\
s.t.\ & \rho(\tilde{\mathbf{s}}) \le \gamma,
\end{aligned} \tag{18}$$

which has employed the same treatment for the bandwidth constraint in (11). The solution $\tilde{\mathbf{s}}^{(k+1)}$ can be found by solving

$$\begin{aligned}
&\min_{\tilde{\mathbf{s}}} \ \|\tilde{\mathbf{s}} - \sum_{m=1}^{M} \mathbf{P}_H\left(i\beta_m^{(k)*}\mathbf{y}_{s,m} + \alpha_m^{(k)*}\mathbf{y}_{r,m}\right)\|^2 \\
&s.t.\ \rho(\tilde{\mathbf{s}}) \le \gamma,
\end{aligned} \tag{19}$$

which admits a closed-form solution using the nearest-vector algorithm, as shown in Appendix VI. Furthermore, the solution to c is computed as

$$c^{(k+1)} = \frac{\mathrm{Re}\left\{\sum_{m=1}^{M} \mathbf{P}_H \left(i\mathbf{y}_{s,m}^{\dagger}\beta_m^{(k)} + \mathbf{y}_{r,m}^{\dagger}\alpha_m^{(k)}\right)\tilde{\mathbf{s}}^{(k+1)}\right\}}{\sum_{m=1}^{M}\left(i|\beta_m^{(k)}|^2 + |\alpha_m^{(k)}|^2\right)}. \quad (20)$$

As such, the MLE of $\mathbf{s}$ for fixed $(\alpha_m^{(k)}, \beta_m^{(k)})$ can be written as

$$\mathbf{s}^{(k+1)} = c^{(k+1)}\tilde{\mathbf{s}}^{(k+1)}. \quad (21)$$

We can now obtain the final PARCBC test as

$$\sum_{m=1}^{M}\|\hat{\mathbf{n}}_{0,m}\|^2 - \sum_{m=1}^{M}\|\hat{\mathbf{n}}_{1,m}\|^2 \underset{H_0}{\overset{H_1}{\gtrless}} \xi, \quad (22)$$

where $\hat{\mathbf{n}}_{0,m}$ and $\hat{\mathbf{n}}_{1,m}$ are the estimates of $\mathbf{n}_{0,m}$ and $\mathbf{n}_{1,m}$ by plugging the estimates of $\mathbf{s}$, $\{\alpha_m\}$ and $\{\beta_m\}$ under H_0 and H_1 hypotheses into (10), respectively.

C. PARUPBC DETECTOR UNDER CONSTANT MODULUS CONSTRAINT

The constant modulus constraint is a special case of the PAR constraint where $\rho(\mathbf{s}) = 1$, which is usually the case of phase modulated or frequency modulated signal [31]. Therefore, plugging in the MLEs of the estimated amplitudes in (17) and employing the bandwidth information, the GLRT with the constant modulus constraint can be expressed by

$$\max_{\mathbf{s},\rho(\mathbf{s})=1} \frac{\mathbf{s}^{\dagger}\mathbf{P}_H\mathbf{R}_1\mathbf{P}_H\mathbf{s}}{\mathbf{s}^{\dagger}\mathbf{s}} - \max_{\mathbf{s},\rho(\mathbf{s})=1} \frac{\mathbf{s}^{\dagger}\mathbf{P}_H\mathbf{R}_0\mathbf{P}_H\mathbf{s}}{\mathbf{s}^{\dagger}\mathbf{s}} \underset{H_0}{\overset{H_1}{\gtrless}} \xi. \quad (23)$$

The constant modulus signal $\mathbf{s}$ can be written as $\mathbf{s} = \delta[e^{j\phi_1}, e^{j\phi_2}, \cdots, e^{j\phi_N}]$, where δ is a constant amplitude and ϕ_n, $n = 1, 2, \cdots, N$, denote the phases. There is no closed-form solution to $\mathbf{s}$ that maximizes $\mathbf{s}^{\dagger}\mathbf{P}_H\mathbf{R}_i\mathbf{P}_H\mathbf{s}$ under the constant modulus constraint. We resort to an upper bound to approach the maximum objective function, which is given by

$$\begin{aligned}\mathbf{s}^{\dagger}\mathbf{P}_H\mathbf{R}_i\mathbf{P}_H\mathbf{s} &= \sum_{p,q=1}^{N} r_{p,q}e^{j(\phi_p-\phi_q)} \\ &\le \|\mathbf{P}_H\mathbf{R}_i\mathbf{P}_H\|_1, \end{aligned} \quad (24)$$

where $r_{p,q}$ denotes the (p,q)-th entry of $\mathbf{P}_H\mathbf{R}_i\mathbf{P}_H$, and $\|\mathbf{P}_H\mathbf{R}_i\mathbf{P}_H\|_1 = \sum_{p,q=1}^{N}|r_{p,q}|$, we have assumed $\delta = 1$ for simplification, and the equality holds if and only if there exists

$$\phi_p - \phi_q = -\arg(r_{p,q}) \quad (25)$$

here $\arg(\cdot)$ means argument. This way, the approximate GLRT for the constant modulus signal is given by

$$\|\mathbf{P}_H\mathbf{R}_1\mathbf{P}_H\|_1 - \|\mathbf{P}_H\mathbf{R}_0\mathbf{P}_H\|_1 \underset{H_0}{\overset{H_1}{\gtrless}} \xi, \quad (26)$$

where the test utilizes an upper bound of $\mathbf{s}^{\dagger}\mathbf{P}_H\mathbf{R}_i\mathbf{P}_H\mathbf{s}$ and we name it as the PARupBC test.

D. PARLOBC DETECTOR UNDER CONSTANT MODULUS CONSTRAINT

Another feasible approximation is based on rank-1 approximation which provides a lower bound for each of the maximization problem. Exploiting the fact that

$$\begin{aligned}\max_{\mathbf{s},\rho(\mathbf{s})=1} \mathbf{s}^{\dagger}\mathbf{P}_H\mathbf{R}_i\mathbf{P}_H\mathbf{s} &\ge \max_{\mathbf{s},\rho(\mathbf{s})=1} \lambda_{max}(\mathbf{P}_H\mathbf{R}_i\mathbf{P}_H)\mathbf{s}^{\dagger}\mathbf{u}_i\mathbf{u}_i^{\dagger}\mathbf{s} \\ &= \lambda_{max}(\mathbf{P}_H\mathbf{R}_i\mathbf{P}_H)\|\mathbf{u}_i\|_1^2, \end{aligned} \quad (27)$$

where $\mathbf{u}_i$ is the principal eigenvector of $\mathbf{P}_H\mathbf{R}_i\mathbf{P}_H$, we can obtain a lower bound-based test with the constant modulus constraint (PARloBC) as

$$\lambda_{max}(\mathbf{P}_H\mathbf{R}_1\mathbf{P}_H)\|\mathbf{u}_1\|_1^2 - \lambda_{max}(\mathbf{P}_H\mathbf{R}_0\mathbf{P}_H)\|\mathbf{u}_0\|_1^2 \underset{H_0}{\overset{H_1}{\gtrless}} \xi. \quad (28)$$

Remark 2: Specially, the PARloBC method in the monostatic case with $M = 1$ suffers from heavy computations with $N \times N$ matrix eigenvalue decomposition. To alleviate this problem, some matrix manipulations are adopted to obtain the final test as

$$\frac{1}{\lambda_1}\|[\tilde{\mathbf{y}}_r', \tilde{\mathbf{y}}_s']\mathbf{v}_1\|_1^2 - \|\tilde{\mathbf{y}}_r'\|^2\|\tilde{\mathbf{y}}_r'\|_1^2 \underset{H_0}{\overset{H_1}{\gtrless}} \xi, \quad (29)$$

where

$$\tilde{\mathbf{y}}_r' = \mathbf{P}_H\tilde{\mathbf{y}}_r, \quad \tilde{\mathbf{y}}_s' = \mathbf{P}_H\tilde{\mathbf{y}}_s, \quad (30)$$

$$\lambda_1 = \frac{1}{2}\left(\|\tilde{\mathbf{y}}_r'\|^2 + \|\tilde{\mathbf{y}}_s'\|^2 + \sqrt{(\|\tilde{\mathbf{y}}_r'\|^2 - \|\tilde{\mathbf{y}}_s'\|^2)^2 - 4|\tilde{\mathbf{y}}_s'^{\dagger}\tilde{\mathbf{y}}_r'|^2}\right), \quad (31)$$

$$\mathbf{v}_1 = [\lambda_1 - \|\tilde{\mathbf{y}}_s'\|^2, 2\tilde{\mathbf{y}}_s'^{\dagger}\tilde{\mathbf{y}}_r']^T. \quad (32)$$

The details are given in Appendix C.

IV. DETECTORS FOR SEVERAL DEGRADED CASES

This section discusses several degraded cases where only part of the prior knowledge is available and proposes the corresponding detectors. Furthermore, the challenge of undetermined bandwidth is tackled by using the SBL algorithm.

A. GLRT WITH PAR CONSTRAINT ONLY

In this sub-section, we derive several GLRT detectors that consider only the PAR constraint, following the derivations of the GLRT detectors in the previous section. The key problem is to estimate the unknown signal under this constraint.

1) PARP DETECTOR

Employing the same technique as in Algorithm 1, a new detector (named the PARP detector) can be obtained, which has the same form as (16) but applies a different estimator

$$\begin{aligned}&\min_{\mathbf{s}} \ \mathbf{s}^{\dagger}\mathbf{R}_i\mathbf{s} \\ &\text{s.t. } \rho(\mathbf{s}) \le \gamma, \quad \|\mathbf{s}\|^2 = 1. \end{aligned} \quad (33)$$

2) PARC DETECTOR

In addition, following Algorithm 2 of the PARCBC method, the optimization problem (18) under the PAR constraint only (named the PARC) can be formulated as

$$\begin{aligned}\min_{\tilde{\mathbf{s}},c}\ & -2\sqrt{c}Re\left\{\sum_{m=1}^{M}\left(i\mathbf{y}_{s,m}^{\dagger}\beta_m^{(k)}+\mathbf{y}_{r,m}^{\dagger}\alpha_m^{(k)}\right)\tilde{\mathbf{s}}\right\}\\ &+\sum_{m=1}^{M}\left(i|\beta_m^{(k)}|^2+|\alpha_m^{(k)}|^2\right)c\\ \text{s.t. }&\rho(\tilde{\mathbf{s}})\le\gamma.\end{aligned}\tag{34}$$

Substituting the estimates of $\mathbf{s}$ into the GLRT form yields the same test as (22) with different estimators.

3) PARLO DETECTOR

For the detection of a constant modulus signal, we may use the same approximation in (26) and obtain the PARlo detector, i.e.,

$$\|\mathbf{R}_1\|_1-\|\mathbf{R}_0\|_1\underset{H_0}{\overset{H_1}{\gtrless}}\xi.\tag{35}$$

4) PARUP DETECTOR

Similarly, the PARup method under the constant envelope signal condition can be recast as

$$\lambda_{max}(\mathbf{R}_1)\|\tilde{\mathbf{u}}_1'\|_1^2-\lambda_{max}(\mathbf{R}_0)\|\tilde{\mathbf{u}}_0'\|_1^2\underset{H_0}{\overset{H_1}{\gtrless}}\xi,\tag{36}$$

where $\tilde{\mathbf{u}}_i'$ denotes the principal eigenvector of $\mathbf{R}_i$.

B. GLRT WITH BANDWIDTH CONSTRAINT ONLY

In this subsection, we consider detectors that assume only the constraint on the bandwidth. Similarly, resorting to the GLRT framework, the problem can be recast as

$$\min_{\boldsymbol{\alpha},\mathbf{s}\in R(\mathbf{H})}\sum_{m=1}^{M}\|\mathbf{n}_0\|^2-\min_{\boldsymbol{\alpha},\boldsymbol{\beta},\mathbf{s}\in R(\mathbf{H})}\sum_{m=1}^{M}\|\mathbf{n}_1\|^2\underset{H_0}{\overset{H_1}{\gtrless}}\xi.\tag{37}$$

The test statistics can be expressed by

$$\lambda_{max}(\mathbf{P}_H\mathbf{R}_1\mathbf{P}_H)-\lambda_{max}(\mathbf{P}_H\mathbf{R}_0\mathbf{P}_H)\underset{H_0}{\overset{H_1}{\gtrless}}\xi,\tag{38}$$

which is derived in Appendix VI. We name the resulting detector the bandwidth constraint (BC) detector.

Remark 3: Specially, for the momostatic case, i.e., $M=1$, we can get

$$\lambda_{max}(\mathbf{P}_H\mathbf{R}_0\mathbf{P}_H)=\|\mathbf{P}_H\tilde{\mathbf{y}}_r\|^2\tag{39}$$

under H_0 hypothesis, and

$$\begin{aligned}&\lambda_{max}(\mathbf{P}_H\mathbf{R}_1\mathbf{P}_H)\\ &=\lambda_{max}(\mathbf{P}_H(\tilde{\mathbf{y}}_r\tilde{\mathbf{y}}_r^{\dagger}+\tilde{\mathbf{y}}_s\tilde{\mathbf{y}}_s^{\dagger})\mathbf{P}_H)\\ &=\frac{1}{2}\big(\|\mathbf{P}_H\tilde{\mathbf{y}}_r\|^2+\|\mathbf{P}_H\tilde{\mathbf{y}}_s\|^2\\ &\quad+\sqrt{(\|\mathbf{P}_H\tilde{\mathbf{y}}_r\|^2-\|\mathbf{P}_H\tilde{\mathbf{y}}_s\|^2)^2-4|\tilde{\mathbf{y}}_s^{\dagger}\mathbf{P}_H\tilde{\mathbf{y}}_r|^2}\big).\end{aligned}\tag{40}$$

for the H_1 hypothesis. In this case, the BC detector can be expressed by

$$\begin{aligned}&\|\mathbf{P}_H\tilde{\mathbf{y}}_s\|^2-\|\mathbf{P}_H\tilde{\mathbf{y}}_r\|^2\\ &\quad+\sqrt{(\|\mathbf{P}_H\tilde{\mathbf{y}}_r\|^2-\|\mathbf{P}_H\tilde{\mathbf{y}}_s\|^2)^2-4|\tilde{\mathbf{y}}_s^{\dagger}\mathbf{P}_H\tilde{\mathbf{y}}_r|^2}\underset{H_0}{\overset{H_1}{\gtrless}}\xi.\end{aligned}\tag{41}$$

C. GLRT WITH UNKNOWN BANDWIDTH

In the previous discussion, it is assumed that the frequency range of the unknown signal is known and the bandpass filter, i.e., the Fourier matrix $\mathbf{H}$, has a passband of the same frequency range. In this sub-section, we assume that the frequency band of the signal is unknown. We employ a Bayesian model to estimate the unknown signal, which encourages the sparsity in the frequency domain and automatically tunes the filter passband.

Now the GLRT problem with an unknown frequency range is formulated as

$$\begin{aligned}\min_{\boldsymbol{\alpha},\mathbf{s}}\ &\sum_{m=1}^{M}\|\mathbf{n}_{0,m}\|^2\\ \text{s.t. }&\mathbf{s}\boldsymbol{\alpha}^T=\bar{\mathbf{H}}\bar{\mathbf{X}}_0\\ &\|\bar{\mathbf{X}}_{0,m}\|_0=B,\end{aligned}\tag{42}$$

and,

$$\begin{aligned}\min_{\boldsymbol{\alpha},\boldsymbol{\beta},\mathbf{s}}\ &\sum_{m=1}^{M}\|\mathbf{n}_{1,m}\|^2\\ \text{s.t. }&\mathbf{s}[\boldsymbol{\alpha}^T,\boldsymbol{\beta}^T]=\bar{\mathbf{H}}\bar{\mathbf{X}}_1\\ &\|\bar{\mathbf{X}}_{1,m}\|_0=B,\end{aligned}\tag{43}$$

where the overcomplete dictionary matrix

$$\bar{\mathbf{H}}=[\mathbf{a}(f_1),\mathbf{a}(f_2),\ldots,\mathbf{a}(f_D)]\in\mathbb{C}^{N\times D}\tag{44}$$

has a dimension of $D\gg N$, and the total number of non-zero elements of each column of the Fourier coefficient matrix $\bar{\mathbf{X}}$ equals to the bandwidth B. The response due to the opportunity signal in the received signals can be represented by $\bar{\mathbf{H}}\bar{\mathbf{X}}_i$, where $\bar{\mathbf{X}}_0\in\mathbb{C}^{D\times M}$ and $\bar{\mathbf{X}}_1\in\mathbb{C}^{D\times 2M}$ are the unknown coefficient matrices under hypotheses H_i, $i=0,1$. Note that the columns of the sparse matrix $\bar{\mathbf{X}}_i$ share the same support (i.e., the same indexes of nonzeros entries). We can thus apply techniques for common sparsity recovery [32] to estimate $\bar{\mathbf{X}}_i$.

The GLRT problem is now tackled by solving two minimization problems $\min_{\boldsymbol{\alpha},i\boldsymbol{\beta},\mathbf{s}}\sum_{m=1}^{M}\|\mathbf{n}_{i,m}\|^2$ under H_i, $i=0,1$, i.e.,

$$\hat{\bar{\mathbf{X}}}_i=\arg\min_{\bar{\mathbf{X}}_i}\|\mathbf{Y}_i-\bar{\mathbf{H}}_i\bar{\mathbf{X}}_i\|_F^2,\tag{45}$$

where the measurement matrices are

$$\mathbf{Y}_1=\left[\tilde{\mathbf{Y}}_r,\tilde{\mathbf{Y}}_s\right]\in\mathbb{C}^{N\times 2M}\quad\text{and }\mathbf{Y}_0=\tilde{\mathbf{Y}}_r\in\mathbb{C}^{N\times M}.\tag{46}$$

We assume that all the rows of $\bar{\mathbf{X}}_i$, denoted by $\bar{\mathbf{X}}_{i,m}$ are mutually independent with the Gaussian density, given by

$$p\left(\bar{\mathbf{X}}_{i,m};\gamma_m,\mathbf{B}_m\right)\sim N\left(\mathbf{0},\gamma_m\mathbf{B}_m\right),\tag{47}$$

TABLE 1. Test statistics under various prior knowledge.

Abbreviation	Test Statistics	Prior Knowledge
BC	$\lambda_{max}(\mathbf{P}_H\mathbf{R}_1\mathbf{P}_H) - \lambda_{max}(\mathbf{P}_H\mathbf{R}_0\mathbf{P}_H)$	Bandwidth
BSBL	$\|\mathbf{Y}_0 - \bar{\mathbf{H}}_0\hat{\bar{\mathbf{X}}}_0\|_F^2 - \|\mathbf{Y}_1 - \bar{\mathbf{H}}_1\hat{\bar{\mathbf{X}}}_1\|_F^2$	None
PARP	$\frac{\hat{\mathbf{s}}_1^\dagger\mathbf{R}_1\hat{\mathbf{s}}_1}{\hat{\mathbf{s}}_1^\dagger\hat{\mathbf{s}}_1} - \frac{\hat{\mathbf{s}}_0^\dagger\mathbf{R}_0\hat{\mathbf{s}}_0}{\hat{\mathbf{s}}_0^\dagger\hat{\mathbf{s}}_0}$	PAR
PARC	$\sum_{m=1}^{M}\|\hat{\mathbf{n}}_{0,m}\|^2 - \sum_{m=1}^{M}\|\hat{\mathbf{n}}_{1,m}\|^2$	PAR
PARup	$\|\mathbf{R}_1\|_1 - \|\mathbf{R}_0\|_1$	Constant modulus
PARlo	$\lambda_{max}(\mathbf{R}_1)\|\mathbf{u}_1'\|_1^2 - \lambda_{max}(\mathbf{R}_0)\|\mathbf{u}_0'\|_1^2$	Constant modulus
PARPBC	$\frac{\hat{\mathbf{s}}_1^\dagger\mathbf{P}_H\mathbf{R}_1\mathbf{P}_H\hat{\mathbf{s}}_1}{\hat{\mathbf{s}}_1^\dagger\hat{\mathbf{s}}_1} - \frac{\hat{\mathbf{s}}_0^\dagger\mathbf{P}_H\mathbf{R}_0\mathbf{P}_H\hat{\mathbf{s}}_0}{\hat{\mathbf{s}}_0^\dagger\hat{\mathbf{s}}_0}$	PAR and bandwidth
PARCBC	$\sum_{m=1}^{M}\|\hat{\mathbf{n}}_{0,m}\|^2 - \sum_{m=1}^{M}\|\hat{\mathbf{n}}_{1,m}\|^2$	PAR and bandwidth
PARupBC	$\lambda_{max}(\mathbf{P}_H\mathbf{R}_1\mathbf{P}_H)\|\tilde{\mathbf{u}}_1\|_1^2 - \lambda_{max}(\mathbf{P}_H\mathbf{R}_0\mathbf{P}_H)\|\tilde{\mathbf{u}}_0\|_1^2$	Constant modulus and bandwidth
PARloBC	$\|\mathbf{P}_H\mathbf{R}_1\mathbf{P}_H\|_1 - \|\mathbf{P}_H\mathbf{R}_0\mathbf{P}_H\|_1$	Constant modulus and bandwidth

where $m = 1, \ldots, M$, for $i = 0, m = 1, \ldots, 2M$, for $i = 1$, γ_m is a nonnegative hyperparameter controlling the sparsity of $\bar{\mathbf{X}}_i$, and $\mathbf{B}_m$ is an unknown positive definite matrix capturing the correlation structure of each $\bar{\mathbf{X}}_{i,m}$. Herein, we adopt the block sparse Bayesian learning (BSBL) algorithm to solve (45) and also learn the hyperparameter γ_m and the correlation matrices $\mathbf{B}_m$ [32]–[34]. Finally, plugging in the solutions of (45) into the GLRT, we can obtain the final test

$$\|\mathbf{Y}_0 - \bar{\mathbf{H}}_0\hat{\bar{\mathbf{X}}}_0\|_F^2 - \|\mathbf{Y}_1 - \bar{\mathbf{H}}_1\hat{\bar{\mathbf{X}}}_1\|_F^2 \underset{H_0}{\overset{H_1}{\gtrless}} \xi. \tag{48}$$

V. NUMERICAL RESULTS

This section presents numerical results to evaluate the performance of the proposed detectors. The test statistics for different prior knowledge are listed in Table 1. We also compare the proposed detectors with the CC detector given by (2), the generalized canonical correlation (GCC) detector (with knowledge of the noise power) in [13], and the GLRT-based constant false alarm rate (GBC) detection in [10].

A. SIMULATION SCENARIO

For a fair comparison, we set the simulation setup of [13]. In addition, three kinds of signals are adopted in this sections.

1) SIGNAL WITH BANDWIDTH CONSTRAINT

Set $\mathbf{x} \in \mathbb{C}^{B\times 1}$ is sampled from $\mathcal{CN}(\mathbf{0}, \mathbf{I})$. The signal $\mathbf{s}$ transmitted from the IO is modeled as

$$\mathbf{s} = \frac{\mathbf{H}\mathbf{x}}{\|\mathbf{H}\mathbf{x}\|}, \tag{49}$$

where $\mathbf{H} \in \mathbb{C}^{H\times B}$ is the known bandwidth Fourier matrix.

2) SIGNAL WITH PAR CONSTRAINT

We assume the signal $\mathbf{s}$ is sampled from

$$\begin{aligned} &\text{find } \mathbf{s} \\ &\text{s.t. } |\mathbf{s}(n)| \le \gamma, \quad n = 1, \cdots, N \\ &\quad \|\mathbf{s}\|^2 = 1, \end{aligned} \tag{50}$$

where $\gamma = \sqrt{N\rho(\mathbf{s})}$. The solution of this problem can be developed by the algorithm in [35], where the solutions are random by random initial value. For the constant modulus signal condition, the transmit signals are chosen as $\mathbf{s} = \delta[e^{j\phi_1}, e^{j\phi_2}, \cdots, e^{j\phi_N}]$.

3) SIGNAL WITH BANDWIDTH AND PAR CONSTRAINT

We assume the signal $\mathbf{s}$ is sampled from

$$\begin{aligned} &\text{find } \mathbf{x} \\ &\text{s.t. } |\mathbf{s}(n)| \le \gamma, \quad n = 1, \cdots, N \\ &\quad \|\mathbf{s}\|^2 = 1 \\ &\quad \mathbf{s} = \mathbf{H}\mathbf{x}, \end{aligned} \tag{51}$$

Similarly, the output of this problem can be solved by the algorithm in [35].

We consider a multistatic passive radar network with one transmitting station and $M = 3$ receiving stations, where each receiving station possesses collocated reference and surveillance antennas. Similar in [13], the reference and surveillance channels noise are drawn from $\mathcal{CN}(\mathbf{0}, \sigma_r^2\mathbf{I})$ and $\mathcal{CN}(\mathbf{0}, \sigma_s^2\mathbf{I})$, respectively. We fix $\|\mathbf{s}\|^2 = 1$. Under each hypothesis, the signal-to-noise ratio (SNR) of the received signal from the RP is given by

$$\mathrm{SNR}_{\mathrm{RP}} = \frac{\sum_{m=1}^{M}|\alpha_m|^2}{M\sigma^2}. \tag{52}$$

For the SP signal, a similar SNR is defined as

$$\mathrm{SNR}_{\mathrm{SP}} = \frac{\sum_{m=1}^{M}|\beta_m|^2}{M\sigma^2}. \tag{53}$$

We fix $\mathrm{SNR}_{\mathrm{RP}} = 5$dB and different values of $\mathrm{SNR}_{\mathrm{SP}}$ are considered. In the following, $\mathrm{SNR}_{\mathrm{SP}}$ will be abbreviated as SNR. The probability of false alarm is set to $P_{fa} = 10^{-3}$ and the number of independent trials is chosen to be 10^5. α_m and β_m are scaled to achieve the desired $\mathrm{SNR}_{\mathrm{RP}}$ and $\mathrm{SNR}_{\mathrm{SP}}$. We show below the performance of the proposed detectors under different constraints on the signal.

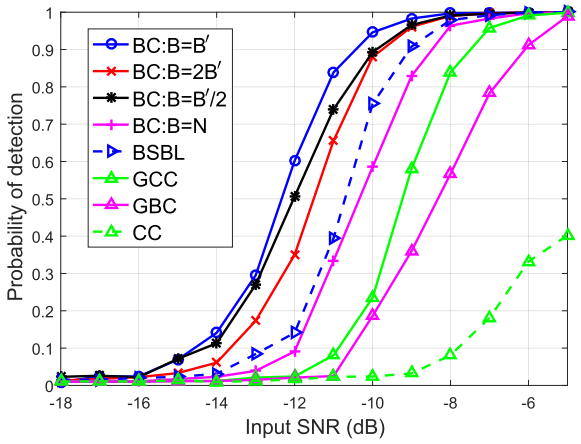

FIGURE 2. Probability of detection versus SNR with $N = 64$ and the true bandwidth $B' = 8$.

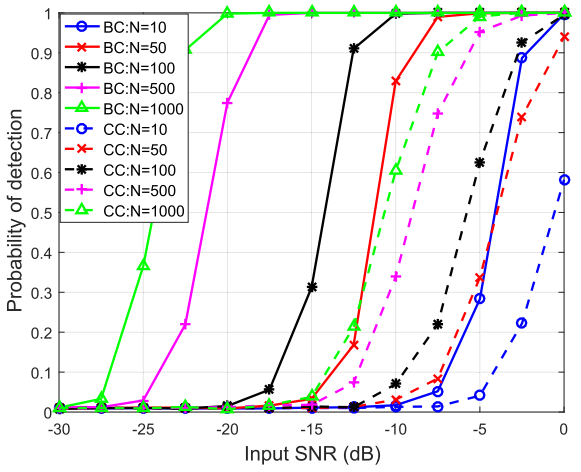

FIGURE 3. Probability of detection versus SNR with different N and the prior bandwidth $B = B' = N/10$.

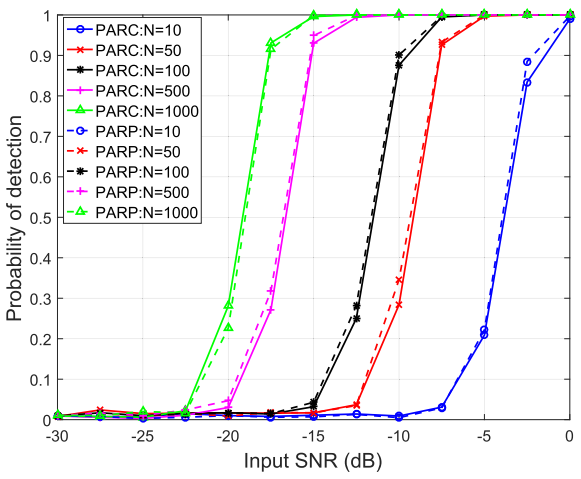

FIGURE 4. Probability of detection versus SNR with the prior PAR knowledge $\rho \leq 1.2$ and different N.

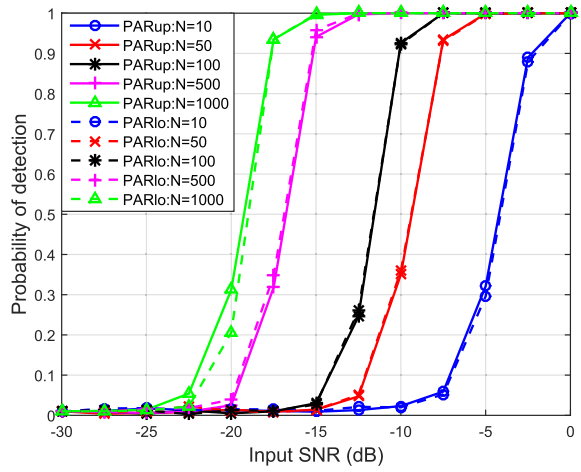

FIGURE 5. Probability of detection versus SNR with the prior PAR knowledge $\rho = 1$ and different N.

B. BANDWIDTH CONSTRAINT

Fig. 2 shows an example with the bandwidth constraint. The number of samples N is 64, the true bandwidth is $B' = 8$, and the normalized bandwidth is $B'/N = 0.125$. The results with bandpass filter $\mathbf{P}_H$ of different bandwidths B are presented. It is seen that the best performance is achieved when the knowledge of the bandwidth is perfect, i.e., $B = B'$. Performance loss can be observed when the knowledge of the bandwidth is imperfect, i.e., $B \neq B'$. The BSBL-based detector, which learns the bandwidth from the data, outperforms the BC detector that sets $B = N$. In addition, all the detectors above outperform the traditional GCC, GBC and CC detectors which do not exploit any prior information about signal.

Fig. 3 demonstrates the influence of the number of samples on the detection performance. Accurate knowledge of the bandwidth, i.e., $B = B' = N/10$, is assumed for the CC detector with different numbers of samples. It is shown that as the number of samples increases, the detection performance improves. In addition, the proposed BC detector significantly outperforms the CC method, especially when the number of samples is large.

C. PAR CONSTRAINT

Fig. 4 shows the detection performance with the prior knowledge of PAR. Two detectors, i.e., the PARC and PARP, are compared under the prior knowledge $\rho \leq 1.2$ for different N. It is shown that the performances of the two detectors PARC and PARP are similar and improve when the number of sample data increases.

Fig. 5 shows the case of constant modulus signals, i.e., $\rho = 1$. Adopting the constant modulus constraint, the PARup and PARlo detectors are examined for different numbers of samples N. It is shown that the two detectors achieve similar performance. Comparisons between Fig. 4 and Fig. 5 reveal that all considered detectors achieve similar detection performance with different N. However, in the constant modulus case, the PARup and PARlo methods require fewer computations as compared to the iteration-based PARC and PARP detectors.

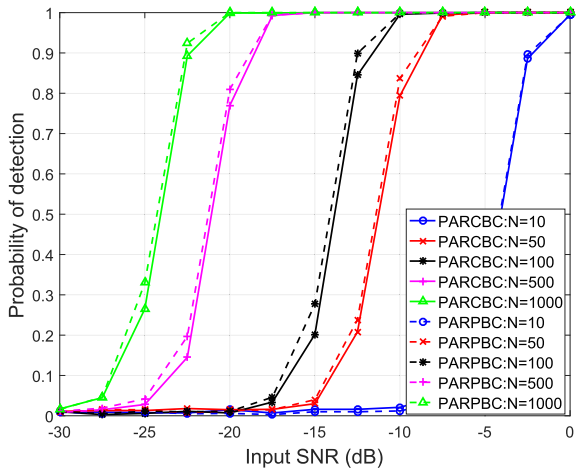

FIGURE 6. Probability of detection versus SNR with the prior knowledge $B = B' = N/10$ and $\rho \leq 1.2$ for different N.

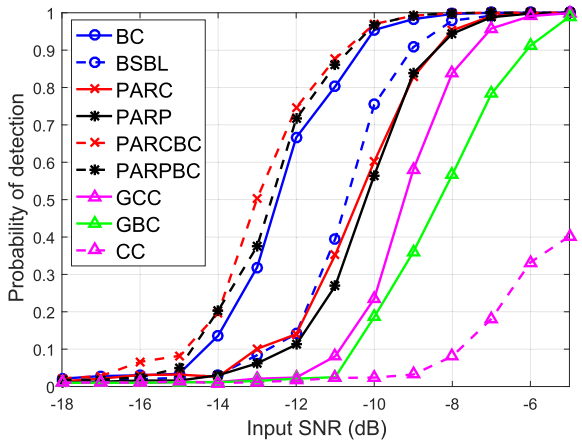

FIGURE 7. Probability of detection versus SNR with the prior knowledge $B = B' = 8$ and $\rho \leq 1.2$ for $N = 64$.

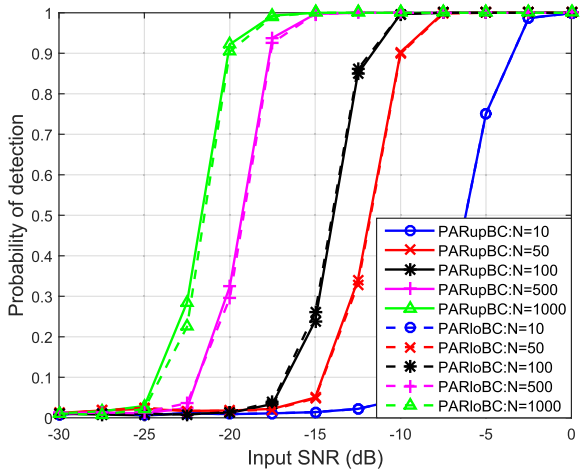

FIGURE 8. Probability of detection versus SNR with the prior knowledge $B = B' = N/10$ and $\rho = 1$ for different N.

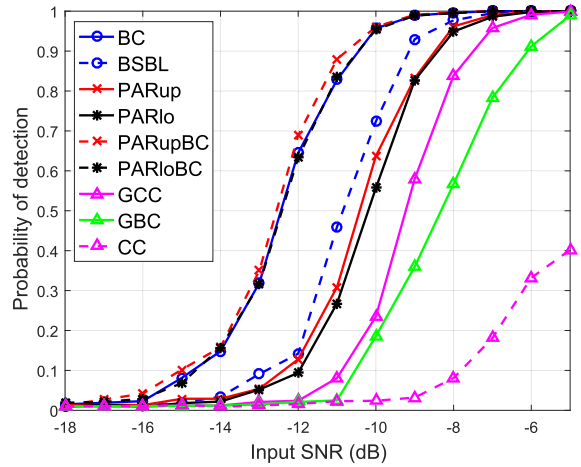

FIGURE 9. Probability of detection versus SNR with the prior knowledge $B = B' = 8$ and $\rho = 1$ for $N = 64$.

D. BANDWIDTH AND PAR CONSTRAINTS

Fig. 6 to Fig. 9 demonstrate examples where the prior knowledge of the bandwidth and PAR are exploited simultaneously. In Fig. 6 and 7, the PARCBC and PARPBC algorithms are considered for an example of $\rho \leq 1.2$. From Fig. 6, the two detectors have similar performance for different N. Fig. 7 demonstrates that our proposed detectors are able to exploit the prior knowledge about the bandwidth and PAR to improve the performance. Similarly, in Fig. 8, the PARupBC and PARloBC detectors are compared for constant modulus signals. Besides, Fig. 9 shows that both detectors can improve the performance when both the PAR and constant modulus knowledge are exploited.

The results in Fig. 7 and 9 indicate that the prior knowledge of the bandwidth is more effective in improving the performance as compared to the PAR knowledge. In order to examine the effect of different constraints, the performance of estimating the unknown signal is depicted in Fig. 10, where one signal plus noise model $\mathbf{s}_r = \alpha\mathbf{s} + \mathbf{w}$ is considered with $\|\mathbf{s}\|^2 = 1$. In particular, the bandwidth-constrained estimator is given by the principal eigenvector $\mathbf{P}_H \mathbf{s}_r \mathbf{s}_r^\dagger \mathbf{P}_H$. The estimator under only the PAR constraint is given by (33) and that under both constraints is given by (14). We can see that the bandwidth constraint plays a more significant role in the signal estimation which can eliminate a majority of the influence of the noise. The PAR knowledge can further suppress the high-power noise. Clearly, exploiting both knowledge can obtain the most significant performance.

E. INACCURATE NOISE POWER ASSUMPTION

In this section, we examine an inaccurate noise power condition, where we set that σ_r^2 and σ_s^2 are not equal. Besides, the passive radar system assume the inaccurate noise power as $\sigma_r^2 = \sigma_s^2 = 1$. Other parameters in the simulation are same as condition of Fig. 7.

Fig. 11 shows detection performances of different detectors under $\sigma_r^2 = 1$ and $\sigma_s^2 = 2$. Similarly, Fig. 12 is examined under $\sigma_r^2 = 2$ and $\sigma_s^2 = 3$ condition. Compared with Fig. 7,

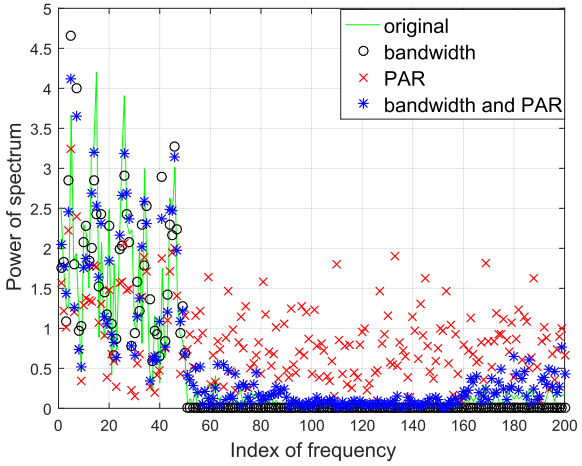

FIGURE 10. Power spectrum with different constraints under SNR $= -10$dB, $N = 200$, the bandwidth $B' = 50$, and $\rho \leq 1.2$.

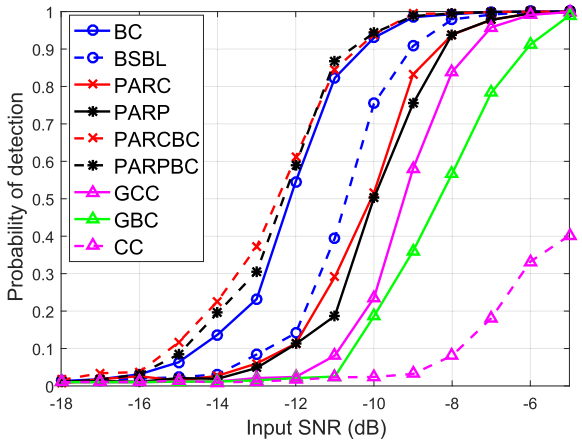

FIGURE 11. Probability of detection versus SNR under $\sigma_r^2 = 1$ and $\sigma_s^2 = 2$ condition, with the prior knowledge $B = B' = 8$ and $\rho \leq 1.2$ for $N = 64$.

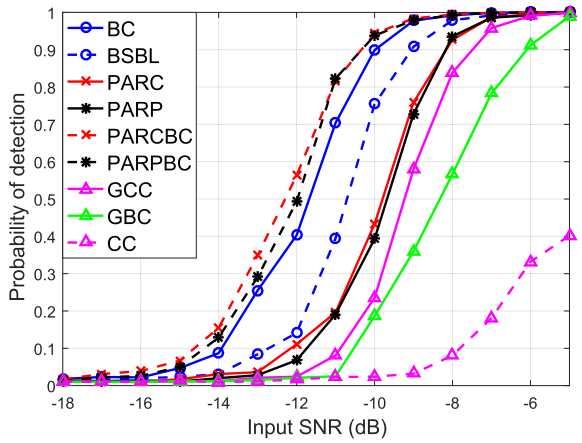

FIGURE 12. Probability of detection versus SNR under $\sigma_r^2 = 2$ and $\sigma_s^2 = 3$ condition, with the prior knowledge $B = B' = 8$ and $\rho \leq 1.2$ for $N = 64$.

the performances of the proposed detectors are degraded. But, it is also shown that the proposed detectors have significant performance than others under inaccurate noise power condition.

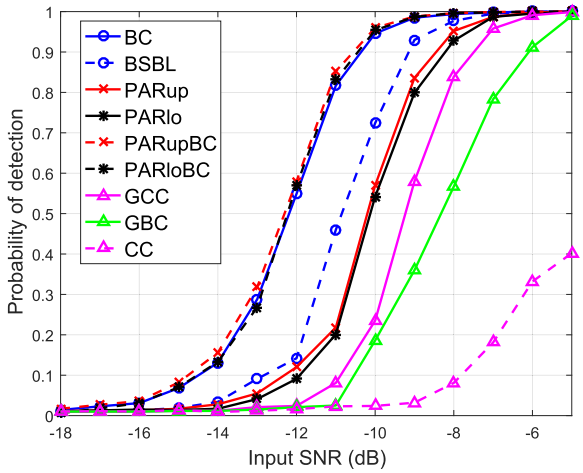

FIGURE 13. Probability of detection versus SNR under $\sigma_r^2 = 1$ and $\sigma_s^2 = 2$ condition, with the prior knowledge $B = B' = 8$ and $\rho = 1$ for $N = 64$.

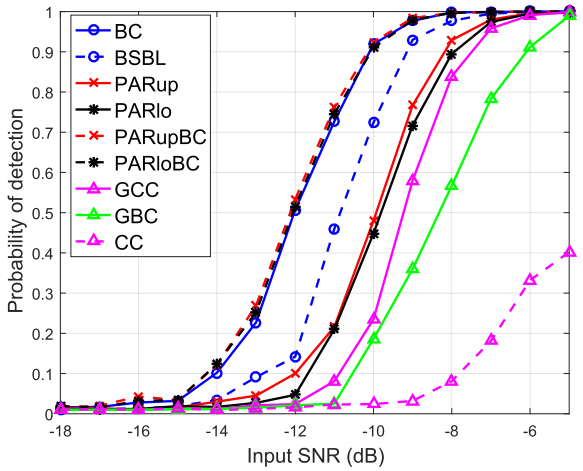

FIGURE 14. Probability of detection versus SNR under $\sigma_r^2 = 2$ and $\sigma_s^2 = 3$ condition, with the prior knowledge $B = B' = 8$ and $\rho = 1$ for $N = 64$.

Under constant modulus condition, Fig. 13 and Fig. 14 present inaccurate noise power condition as $\sigma_r^2 = 1, \sigma_s^2 = 2$ and $\sigma_r^2 = 2, \sigma_s^2 = 3$. Although the proposed detectors have degraded performances, it is also shown that the proposed detectors have better performance than others without prior knowledge.

VI. CONCLUSIONS

In this paper, we investigated the detection problem for multistatic passive radar with the prior knowledge about the bandwidth and PAR, which may be learnt easily in practice. Exploiting the bandwidth knowledge, we adopted the GLRT approach and developed the BC detector, which achieves significant performance improvement even with imperfect knowledge about the bandwidth. To handle the case of unknown bandwidth, the BSBL-based detector was proposed, which shows similar performance. We also developed several detectors that exploit the PAR knowledge, and studied the

special case of constant modulus signals. We also developed detectors that incorporate the knowledge of the bandwidth and PAR simultaneously, which offer further gains in the detection performance.

APPENDIX A PROOF OF (11) AND (38)

First, we present the MLEs of the unknown amplitudes and signal under both hypotheses. The MLEs of β_m and α_m conditioned on $\mathbf{s}$ can be calculated as

$$\hat{\beta}_m = \frac{\mathbf{s}^\dagger \mathbf{y}_{s,m}}{\mathbf{s}^\dagger \mathbf{s}}, \quad \hat{\alpha}_m = \frac{\mathbf{s}^\dagger \mathbf{y}_{r,m}}{\mathbf{s}^\dagger \mathbf{s}}, \tag{54}$$

where $\hat{\beta}_m$ is used for H_1 hypothesis only, and $\hat{\alpha}_m$ for both H_1 and H_0 hypotheses. Substituting (54) into (9), we can obtain a new test conditioned on $\mathbf{s}$:

$$\max_{\mathbf{s}\in R(\mathbf{H}),\rho(\mathbf{s})\le\gamma} \sum_{m=1}^{M} \frac{1}{\sigma_m^2}\left(\frac{|\mathbf{y}_{s,m}^\dagger \mathbf{s}|^2}{\mathbf{s}^\dagger\mathbf{s}} + \frac{|\mathbf{y}_{r,m}^\dagger \mathbf{s}|^2}{\mathbf{s}^\dagger\mathbf{s}}\right) - \max_{\mathbf{s}\in R(\mathbf{H}),\rho(\mathbf{s})\le\gamma} \sum_{m=1}^{M} \frac{1}{\sigma_m^2}\left(\frac{|\mathbf{y}_{r,m}^\dagger \mathbf{s}|^2}{\mathbf{s}^\dagger\mathbf{s}}\right) \underset{H_0}{\overset{H_1}{\gtrless}} \xi. \tag{55}$$

For simplicity, the GLRT problem can be reformulated as

$$\max_{\mathbf{s}\in R(\mathbf{H}),\rho(\mathbf{s})\le\gamma} \frac{\mathbf{s}^\dagger \mathbf{R}_1 \mathbf{s}}{\mathbf{s}^\dagger\mathbf{s}} - \max_{\mathbf{s}\in R(\mathbf{H}),\rho(\mathbf{s})\le\gamma} \frac{\mathbf{s}^\dagger \mathbf{R}_0 \mathbf{s}}{\mathbf{s}^\dagger\mathbf{s}} \underset{H_0}{\overset{H_1}{\gtrless}} \xi. \tag{56}$$

Noticing the constraint $\mathbf{s} \in R(\mathbf{H})$ under two hypotheses, the solution is given by

$$\begin{aligned}
&\max_{\mathbf{s}\in R(\mathbf{H}),\rho(\mathbf{s})\le\gamma} \frac{\mathbf{s}^\dagger \mathbf{R}_i \mathbf{s}}{\mathbf{s}^\dagger\mathbf{s}} \\
&= \max_{\mathbf{s}\in R(\mathbf{H}),\rho(\mathbf{s})\le\gamma} \frac{\mathbf{s}^\dagger (\mathbf{P}_H + \mathbf{P}_\mathbf{H}^\perp)\mathbf{R}_i(\mathbf{P}_H + \mathbf{P}_\mathbf{H}^\perp)\mathbf{s}}{\mathbf{s}^\dagger\mathbf{s}} \\
&= \max_{\mathbf{s},\rho(\mathbf{s})\le\gamma} \frac{\mathbf{s}^\dagger \mathbf{P}_H \mathbf{R}_i \mathbf{P}_H \mathbf{s}}{\mathbf{s}^\dagger\mathbf{s}},
\end{aligned} \tag{57}$$

where $\mathbf{P}_H = \mathbf{H}(\mathbf{H}^\dagger\mathbf{H})^{-1}\mathbf{H}^\dagger$ is the projection matrix onto the subspace of the columns of $\mathbf{H}$ and $\mathbf{P}_H^\perp = \mathbf{I} - \mathbf{P}_H$.

We next derive (38) for the case with only the bandwidth constraint, i.e., there is no constraint on the PAR. The maximization problem of (57) becomes a classical Raleigh quotient problem. The solution is given by

$$\max_{\mathbf{s}} \frac{\mathbf{s}^\dagger \mathbf{P}_H \mathbf{R}_i \mathbf{P}_H \mathbf{s}}{\mathbf{s}^\dagger\mathbf{s}} = \lambda_{max}(\mathbf{P}_H \mathbf{R}_i \mathbf{P}_H). \tag{58}$$

Finally, using the MLEs obtained above, the GLRT can be given by

$$\lambda_{max}(\mathbf{P}_H \mathbf{R}_1 \mathbf{P}_H) - \lambda_{max}(\mathbf{P}_H \mathbf{R}_0 \mathbf{P}_H) \underset{H_0}{\overset{H_1}{\gtrless}} \xi, \tag{59}$$

which is the BC detector.

APPENDIX B SOLUTION OF (15) AND (19)

Both of the problems (15) and (19) can be reformulated as

$$\begin{aligned}
&\min_{\mathbf{s}} \ \|\mathbf{s} - \mathbf{t}\|^2 \\
&\text{s.t. } \rho(\mathbf{s}) < \gamma, \quad \|\mathbf{s}\|^2 = 1,
\end{aligned} \tag{60}$$

where $\mathbf{t} = [t[1], t[2], \ldots, t[N]]^T$ is assumed to be measurement data. This is also equivalent to

$$\begin{aligned}
&\max_{\mathbf{s}} \ \sum_{n=1}^{N} |s[n]||t[n]| \\
&\text{s.t. } |s[n]| < \epsilon \\
&\qquad \sum_{n=1}^{N} |s[n]|^2 = 1,
\end{aligned} \tag{61}$$

where the magnitude of $\mathbf{s}$ is considered, and $\epsilon = \sqrt{\gamma/N}$. The phase part of $\mathbf{s}$ is set as

$$\arg(s[n]) = \arg(t[n]) + (2k+1)\pi, \quad \forall k = 0, \pm 1, \ldots. \tag{62}$$

to minimize the objective problem.

Without loss of generality, we assume that $|t[1]| \ge \ldots \ge |t[N]|$, and the number of nonzero elements of $\mathbf{t}$ is l. Then the solution to (61) is as follows [36].

Case 1 ($l\epsilon^2 \le 1$): We set $s[n] = \epsilon$, for $n = 1, \ldots, l$. For $n = l+1, \ldots, N$, we have $\sum_{n=l+1}^{N} |s[n]|^2 = 1 - l\epsilon^2$, and $0 \le |s[n]| \le \epsilon$. Thus, there are multiple solutions to (61) for this case and one of them is given by

$$|s[n]| = \begin{cases} \epsilon, & n = 1, \ldots, l, \\ \sqrt{\dfrac{1 - l\epsilon^2}{N - l}}, & n = l+1, \ldots, N. \end{cases} \tag{63}$$

Case 2 ($l\epsilon^2 > 1$): The solution to (61) is given by

$$|s[n]| = \min\{\beta |t[n]|, \epsilon\}, \tag{64}$$

where

$$\beta \in \{\, \beta | \sum_{n=1}^{N} \min\left\{\beta^2 |t[n]|^2, \epsilon^2\right\} = 1, \quad \beta \in [0, \frac{\epsilon}{\min\{|t[n]| \mid |t[n]| \ne 0\}}] \,\} \tag{65}$$

Since the function $g(\beta) = \sum_{n=1}^{N} \min\left\{\beta^2 |t[n]|^2, \epsilon^2\right\}$ is strictly increasing within $[0, \frac{\epsilon}{\min\{|t[n]| \mid |t[n]| \ne 0\}}]$ and $g(0) = 0$, only one unique β exists. Numerically, the bisection method can be adopted to find the unique β with high accuracy.

Therefore, the solution to (60) is obtained as

$$\mathbf{s} = \mathcal{P}_\mathcal{S}(\mathbf{t}), \tag{66}$$

where

$$\begin{aligned}
\mathcal{P}_\mathcal{S}(\mathbf{t}) = &-\left(\mathbf{1}_{\mathbb{R}^+}(1 - l\epsilon^2)\right)\epsilon \mathbf{u}_l \odot e^{j\arg(\mathbf{t})} \\
&-\left(\mathbf{1}_{\mathbb{R}^-}(1 - l\epsilon^2)\right)\min\{\beta|\mathbf{t}|, \epsilon\mathbf{1}\} \odot e^{j\arg(\mathbf{t})},
\end{aligned} \tag{67}$$

$\min\{\cdot,\cdot\}$, $|\cdot|$ and $e^{j\arg(\cdot)}$ are element-wise operations, and

$$\mathbf{1}_A(x) = \begin{cases} 1, & \text{if } x \in A, \\ 0, & \text{otherwise}, \end{cases} \tag{68}$$

$$\mathbf{u}_m = [\underbrace{1,\ldots,1}_{l}, \underbrace{\sqrt{\frac{1-l\epsilon^2}{N\epsilon^2-l\epsilon^2}},\ldots,\sqrt{\frac{1-l\epsilon^2}{N\epsilon^2-l\epsilon^2}}}_{N-l}]^T. \tag{69}$$

APPENDIX C SOLUTION OF (29)

To derive (29), we should obtain $\lambda_{max}(\mathbf{P}_H\mathbf{R}_1\mathbf{P}_H)$, $\mathbf{u}_1$, $\lambda_{max}(\mathbf{P}_H\mathbf{R}_0\mathbf{P}_H)$, $\mathbf{u}_0$ in the case $M = 1$. In this case, $\mathbf{R}_0 = \tilde{\mathbf{y}}_r\tilde{\mathbf{y}}_r^\dagger$ and $\mathbf{R}_1 = \tilde{\mathbf{y}}_r\tilde{\mathbf{y}}_r^\dagger + \tilde{\mathbf{y}}_s\tilde{\mathbf{y}}_s^\dagger$. Firstly, we can get

$$\lambda_{max}(\mathbf{P}_H\mathbf{R}_0\mathbf{P}_H) = \|\tilde{\mathbf{y}}_r'\|^2, \tag{70}$$

$$\mathbf{u}_0 = \tilde{\mathbf{y}}_r', \tag{71}$$

and

$$\begin{aligned}\lambda_1 &= \lambda_{max}(\mathbf{P}_H\mathbf{R}_1\mathbf{P}_H) \\ &= \frac{1}{2}\left(\|\tilde{\mathbf{y}}_r'\|^2+\|\tilde{\mathbf{y}}_s'\|^2+\sqrt{(\|\tilde{\mathbf{y}}_r'\|^2-\|\tilde{\mathbf{y}}_s'\|^2)^2-4|\tilde{\mathbf{y}}_s'^\dagger\tilde{\mathbf{y}}_r'|^2}\right).\end{aligned} \tag{72}$$

Correspondingly, we can calculate $\mathbf{u}_1$ using the singular value decomposition (SVD) of $\mathbf{Y}_1 = [\tilde{\mathbf{y}}_r', \tilde{\mathbf{y}}_s'] \in \mathbb{C}^{N\times 2}$, i.e.,

$$\mathbf{U}\mathbf{D}\mathbf{V}^\dagger = \mathbf{Y}_1, \tag{73}$$

where the columns of $\mathbf{U} = [\mathbf{u}_1,\ldots,\mathbf{u}_N]$ are the eigenvectors of $\mathbf{Y}_1\mathbf{Y}_1^\dagger$, $\mathbf{D} = [\Sigma, \mathbf{0}] \in \mathbb{C}^{N\times 2}$, $\Sigma = \text{diag}\{\lambda_1, \lambda_2\}$, and $\mathbf{V} = [\mathbf{v}_1, \mathbf{v}_2]$, in which

$$\mathbf{v}_1 = [\lambda_1 - \|\tilde{\mathbf{y}}_s'\|^2, 2\tilde{\mathbf{y}}_s'^\dagger\tilde{\mathbf{y}}_r']^T, \tag{74}$$

$$\mathbf{v}_2 = [\lambda_2 - \|\tilde{\mathbf{y}}_s'\|^2, 2\tilde{\mathbf{y}}_s'^\dagger\tilde{\mathbf{y}}_r']^T. \tag{75}$$

Thus, we have

$$\mathbf{u}_i = \mathbf{Y}_1\frac{\mathbf{v}_i}{\lambda_i}. \tag{76}$$

REFERENCES

[1] G. Fang, J. Yi, X. Wan, Y. Liu, and H. Ke, "Experimental research of multistatic passive radar with a single antenna for drone detection," *IEEE Access*, vol. 6, pp. 33542–33551, 2018.
[2] D. Pastina, F. Colone, T. Martelli, and P. Falcone, "Parasitic exploitation of Wi-Fi signals for indoor radar surveillance," *IEEE Trans. Veh. Technol.*, vol. 64, no. 4, pp. 1401–1415, Apr. 2015.
[3] A. Khalajmehrabadi, N. Gatsis, and D. Akopian, "Structured group sparsity: A novel indoor WLAN localization, outlier detection, and radio map interpolation scheme," *IEEE Trans. Veh. Technol*, vol. 66, no. 7, pp. 6498–6510, Jul. 2017.
[4] G. Cui, J. Liu, H. Li, and B. Himed, "Target detection for passive radar with noisy reference channel," in *Proc. IEEE Radar Conf.*, May 2014, pp. 144–148.
[5] S. Gogineni, P. Setlur, M. Rangaswamy, and R. R. Nadakuditi, "Passive radar detection with noisy reference channel using principal subspace similarity," *IEEE Trans. Aerosp. Electron. Syst.*, vol. 54, no. 1, pp. 18–36, Feb. 2018.
[6] G. K. Chalise and B. Himed, "GLRT detector in single frequency multistatic passive radar systems," *Signal Process.*, vol. 142, pp. 504–512, Jan. 2018.
[7] P. Falcone *et al.*, "Active and passive radar sensors for airport security," in *Proc. Tyrrhenian Workshop Adv. Radar Remote Sens. (TyWRRS)*, Sep. 2012, pp. 314–321.
[8] D. E. Hack, L. K. Patton, B. Himed, and M. A. Saville, "Centralized passive MIMO radar detection without direct-path reference signals," *IEEE Trans. Signal Process.*, vol. 62, no. 11, pp. 3013–3023, Jun. 2014.
[9] F. Colone, D. W. O'Hagan, P. Lombardo, and C. J. Baker, "A multistage processing algorithm for disturbance removal and target detection in passive bistatic radar," *IEEE Trans. Aerosp. Electron. Syst.*, vol. 45, no. 2, pp. 689–722, Apr. 2009.
[10] A. Zaimbashi, M. Derakhtian, and A. Sheikhi, "GLRT-based CFAR detection in passive bistatic radar," *IEEE Trans. Aerosp. Electron. Syst.*, vol. 49, no. 1, pp. 134–159, Jan. 2013.
[11] X. Zhang, H. Li, and B. Himed, "Multistatic detection for passive radar with direct-path interference," *IEEE Trans. Aerosp. Electron. Syst.*, vol. 53, no. 2, pp. 915–925, Apr. 2017.
[12] D. E. Hack, L. K. Patton, B. Himed, and M. A. Saville, "Detection in passive MIMO radar networks," *IEEE Trans. Signal Process.*, vol. 62, no. 11, pp. 2999–3012, Jun. 2014.
[13] L. Jun, H. Li, and B. Himed, "Two target detection algorithms for passive multistatic radar," *IEEE Trans. Signal Process.*, vol. 62, no. 22, pp. 5930–5939, Nov. 2014.
[14] Q. He and R. S. Blum, "The significant gains from optimally processed multiple signals of opportunity and multiple receive stations in passive radar," *IEEE Signal Process. Lett.*, vol. 21, no. 2, pp. 180–184, Feb. 2014.
[15] L. Giubbolini, "A multistatic microwave radar sensor for short range anticollision warning," *IEEE Trans. Veh. Technol.*, vol. 49, no. 6, pp. 2270–2275, Nov. 2000.
[16] R. Amiri, F. Behnia, and M. A. M. Sadr, "Exact solution for elliptic localization in distributed MIMO radar systems," *IEEE Trans. Veh. Technol.*, vol. 67, no. 2, pp. 1075–1086, Feb. 2018.
[17] P. Kumari, J. Choi, N. Gonzalez-Prelcic, and R. W. Heath, Jr., "IEEE 802.11ad-based radar: An approach to joint vehicular communication-radar system," *IEEE Trans. Veh. Technol.*, vol. 67, no. 4, pp. 3012–3027, Apr. 2018.
[18] F. Colone, T. Martelli, and P. Lombardo, "Quasi-monostatic versus near forward scatter geometry in Wifi-based passive radar sensors," *IEEE Sensors J.*, vol. 17, no. 15, pp. 4757–4772, Aug. 2017.
[19] D. Torrieri, *Principles of Spread-Spectrum Communication Systems*. New York, NY, USA: Springer, 2005.
[20] W. Kellermann and W. Granzow, "Analysis of low-PAR modulation schemes for wideband-CDMA," in *Proc. IEEE 5th Int. Symp. Spread Spectr. Techn. Appl.*, Sep. 1998, pp. 314–317.
[21] C. R. Berger, B. Demissie, J. Heckenbach, P. Willett, and S. Zhou, "Signal processing for passive radar using OFDM waveforms," *IEEE J. Sel. Topics Signal Process.*, vol. 4, no. 1, pp. 226–238, Feb. 2010.
[22] P. Chen, C. Qi, L. Wu, and X. Wang, "Estimation of extended targets based on compressed sensing in cognitive radar system," *IEEE Trans. Veh. Technol*, vol. 66, no. 2, pp. 941–951, Feb. 2017.
[23] H. D. Griffiths and C. J. Baker, "Passive coherent location radar systems. Part 1: Performance prediction," *IEE Proc. Radar Sonar Navigat.*, vol. 152, no. 3, pp. 153–159, Jun. 2005.
[24] J. Liu, H. Li, and B. Himed, "On the performance of the cross-correlation detector for passive radar applications," *Signal Process.*, vol. 113, pp. 32–37, Aug. 2015.
[25] J. Liu, H. Li, and B. Himed, "Analysis of cross-correlation detector for passive radar applications," in *Proc. IEEE Radar Conf.*, May 2015, pp. 772–776.
[26] A. K. Karthik and R. S. Blum, "Improved detection performance for passive radars exploiting known communication signal form," *IEEE Signal Process. Lett.*, vol. 25, no. 11, pp. 1625–1629, Nov. 2018.
[27] I. Santamaria, L. L. Scharf, J. Via, H. Wang, and Y. Wang, "Passive detection of correlated subspace signals in two MIMO channels," *IEEE Trans. Signal Process.*, vol. 65, no. 20, pp. 5266–5280, Oct. 2017.
[28] G. Cui, J. Liu, H. Li, and B. Himed, "Signal detection with noisy reference for passive sensing," *Signal Process.*, vol. 108, pp. 389–399, Mar. 2015.
[29] A. De Maio, Y. Huang, M. Piezzo, S. Zhang, and A. Farina, "Design of optimized radar codes with a peak to average power ratio constraint," *IEEE Trans. Signal Process.*, vol. 59, no. 6, pp. 2683–2697, Jun. 2011.
[30] M. Soltanalian and P. Stoica, "Designing unimodular codes via quadratic optimization," *IEEE Trans. Signal Process.*, vol. 62, no. 5, pp. 1221–1234, Mar. 2014.

[31] X. Yu, G. Cui, L. Kong, J. Li, and G. Gui, "Constrained waveform design for colocated MIMO radar with uncertain steering matrices," *IEEE Trans. Aerosp. Electron. Syst.*, vol. 55, no. 1, pp. 356–370, Feb. 2019.
[32] Z. Zhang and B. D. Rao, "Sparse signal recovery with temporally correlated source vectors using sparse Bayesian learning," *IEEE J. Sel. Topics Signal Process.*, vol. 5, no. 5, pp. 912–926, Sep. 2011.
[33] Z. Zhang and B. D. Rao, "Extension of SBL algorithms for the recovery of block sparse signals with intra-block correlation," *IEEE Trans. Signal Process.*, vol. 61, no. 8, pp. 2009–2015, Apr. 2013.
[34] Z. Zhang, L. Xie, and C. Zhang, "Off-grid direction of arrival estimation using sparse Bayesian inference," *IEEE Trans. Signal Process.*, vol. 61, no. 1, pp. 38–43, Jan. 2013.
[35] K. Huang and N. D. Sidiropoulos, "Consensus-ADMM for general quadratically constrained quadratic programming," *IEEE Trans. Signal Process.*, vol. 64, no. 20, pp. 5297–5310, Oct. 2016.
[36] L. Wu, P. Babu, and D. P. Palomar, "Transmit waveform/receive filter design for MIMO radar with multiple waveform constraints," *IEEE Trans. Signal Process.*, vol. 66, no. 6, pp. 1526–1540, May 2018.

GUOHAO SUN was born in Shanxi, China, in 1990. He received the B.S. degree in electrical engineering from the University of Electronic Science and Technology of China (UESTC), in 2014, where he is currently pursuing the Ph.D. degree in signal and information processing. His research interests include space–time adaptive processing, radar target detection, and waveform design.

WEI ZHANG was born in Inner Mongolia, China, in 1983. He received the B.S., M.S., and Ph.D. degrees in electrical engineering from Southwest Jiaotong University and the University of Electronic Science and Technology of China, in 2004, 2008, and 2013, respectively, where he is currently an Associate Professor. His research interests include array processing, millimeter-wave radar, space–time adaptive processing, and MIMO radar signal processing.

JUN TONG received the B.E. and M.E. degrees from the University of Electronic Science and Technology of China (UESTC), in 2001 and 2004, respectively, and the Ph.D. degree in electronic engineering from the City University of Hong Kong, in 2009. He is currently a Senior Lecturer with the School of Electrical, Computer and Telecommunications Engineering, University of Wollongong, Australia. His research interest includes signal processing and its applications to communication systems.

ZISHU HE was born in Chengdu, China, in 1962. He received the B.S., M.S., and Ph.D. degrees in signal and information processing from the University of Electronic Science and Technology of China (UESTC), in 1984, 1988, and 2000, respectively, where he is currently a Professor with the School of Electronic Engineering in signal and information processing. He has finished more than 100 papers and has written two books, one is *Signals and Systems* and another is *Modern Digital Signal Processing and its Applications*. His current research interests include array signal processing, digital beam forming, the theory on MIMO communication and MIMO radar, adaptive signal processing, and channel estimation.

ZHIHANG WANG was born in Fujian, China, in 1993. He received the B.S. degree from the University of Electronic Science and Technology of China (UESTC), Chengdu, China, in 2016, where he is currently pursuing the Ph.D. degree in signal and information processing. His research interests include array signal processing, compressive sensing, radar target detection, and machine learning.